Check for updates

Systematic Raman spectroscopic study of the complexation of uranyl with fluoride†

Yating Yang, [iD] ‡[a] Qian Liu,‡*[a] Youshi Lan,[a] Qianci Zhang,[a] Liyang Zhu,[a] Suliang Yang, [iD][a] Guoxin Tian, [iD][a] Xiaoyan Cao [iD]*[bc] and Michael Dolg [iD]*[bc]

A simple aqueous complexing system of UO_2^{2+} with F^- is selected to systematically illustrate the application of Raman spectroscopy in exploring uranyl(VI) chemistry. Five successive complexes, UO_2F^+, $UO_2F_2(aq)$, $UO_2F_3^-$, $UO_2F_4^{2-}$, and $UO_2F_5^{3-}$, are identified, as well as the formation constants except for the 1:5 species $UO_2F_5^{3-}$, which was experimentally observed here for the first time. The standard relative molar Raman scattering intensity for each species is obtained by deconvolution of the spectra collected during titrations. The results of relativistic quantum chemical first-principles and *ab initio* calculations are presented for the complete set of $[UO_2(H_2O)_mF_n]^{2-n}$ complexes ($n = 0-5$), both for the gas phase as well as for aqueous solution modelling bulk water using the conductor-like screening model. Electronic structure calculations at the Møller–Plesset second-order perturbation theory level provide accurate geometrical parameters and in particular reveal that k water molecules in the second coordination sphere coordinating to the F^- ligands in the resulting $[UO_2(H_2O)_mF_n]^{2-n}(H_2O)_k$ complexes need to be treated explicitly in order to obtain vibrational frequencies in very good agreement with experimental data. The thermodynamics and structural information obtained in this work and the developed methodology could be instructive for the future experimental and computational research on the complexation of the uranyl ion.

1. Introduction

The coordination chemistry and speciation of uranyl in aqueous solutions are of great importance in the nuclear fuel cycle and nuclear waste disposal.[1,2] In the processes of fuel manufacturing and spent nuclear fuel reprocessing, the thermodynamic parameters of uranyl complexes are needed for equipment design and operation control. For the waste disposal, the speciation of uranyl under associated conditions is the base for depicting and controlling the migration of uranium. In addition, to precisely determine the thermodynamic parameters and to get structural information of uranyl complexes are not only important tasks of experimental chemistry, but also help to further develop

[a] *Department of Radiochemistry, China Institute of Atomic Energy, Fangshan District, Beijing, 102413, China. E-mail: liuqian@cnncmail.cn*

[b] *College of Chemistry, Beijing Normal University, Beijing, 100875, China*

[c] *Institute of Theoretical Chemistry, University of Cologne, Greinstr. 4, 50939 Cologne, Germany. E-mail: x.cao@uni-koeln.de, m.dolg@uni-koeln.de*

† Electronic supplementary information (ESI) available: Calculated stepwise formation constants (K_5) of the $UO_2F_5^{3-}$ complex. U=O bond distances and UO_2^{2+} symmetric stretching frequencies calculated for the gas phase/aqueous solution (COSMO) at the B3LYP/MP2 levels, as well as Cartesian coordinates and total energies of the optimized B3LYP equilibrium structures in aqueous solution (COSMO) of selected complexes $[UO_2(H_2O)_mF_n]^{2-n}(H_2O)_k$. See DOI: https://doi.org/10.1039/d4cp01569j

‡ Equal contributions.

analytical techniques and assist in selecting suitable model systems for computational calibration studies. Therefore, to develop methods and procedures for thermodynamically and structurally investigating the complexation and speciation of uranyl are essential to both fundamental research and applications.

A variety of experimental methods can be applied to study the speciation of uranyl, for example, potentiometric titration,[3–5] calorimetric titration,[6–8] separation by ion exchange[9] or solvent extraction,[10,11] as well as spectral titration.[12–14] Therein, among the spectroscopic methods especially Raman spectroscopy shows better adaptability since it is simple to operate, and can provide thermodynamic and structural information at the same time. Till now, a considerable amount of research has been performed to interpret the spectroscopic performances of uranyl single crystals. However, due to the difficulty in characterizing the uranyl speciation in solution caused by the dynamic ligand-solvent coordination complexity, most of the studies exist on the speciation and spectra of uranyl but very few present integrated explications. Drobot recently developed a numerical processing of single-component emission spectra to improve the signal-to-structure correlation.[15,16] Additional information gained enables a cross-validation with Raman spectroscopy, but measurements of the Raman spectra of uranyl single-species were not performed. Hence, applying the nondestructive Raman spectral titration method[14] to investigate the signal-to-structure correlation in uranyl single-species is

18584 | *Phys. Chem. Chem. Phys.*, 2024, **26**, 18584–18591

This journal is © the Owner Societies 2024

necessary. In most inorganic and organic uranyl ligands, the fluoride ion (F^-) has been chosen as a popular target ligand for uranyl research, since it does not show a Raman signal and will not quench the fluorescence of uranyl. Significantly, apart from the other halide ions, F^- exhibits unusual coordination properties due to its high charge density and highly negative free energy of hydration, along with the formation of hydrogen bonds with water molecules in aqueous solution. Hence, complicated and changeable uranyl fluorides exhibit an extreme challenge but also offer a research prospect in structure determination through the Raman spectral titration method as well as the exact exploration of the intrinsic signal-to-structure correlation. Meanwhile, the radiotoxicity of actinides intensively motivates the associated alternative theoretical studies, which can alleviate the hazards of radioactive contamination to the environment and researchers themselves to some extent. What's more, what determines the signal-to-structure correlation is not clear, as well as how to determine the exact energy-favorable configuration in real aqueous solution and precisely describe the solvent effect for uranyl fluorides, which all need further interpretation at the atomic level. Therefore, theoretical and experimental research studies are equally important.

Modern relativistic quantum chemical methods allow a detailed investigation of molecules containing heavy elements both in the gas phase and in solution. In 1999 Schreckenbach et al. published results of gradient-corrected (BLYP)[17] and hybrid (B3LYP)[18] density functional theory (DFT) calculations for $UO_2X_4^{2-}$ (X = F, Cl, OH) and AnF_6 (An = U, Np, Pu) complexes using effective core potentials (ECP) and a quasi-relativistic (QR) all-electron (AE) approach.[19] The calculated symmetric UO_2^{2+} stretching frequencies in $UO_2F_4^{2-}$ of 766 cm^{-1} (QR AE, BLYP), 682 cm^{-1} (ECP, BLYP) and 771 cm^{-1} (ECP, B3LYP) were only in modest agreement with the experimentally observed at least 50 cm^{-1} higher value of 822 cm^{-1} for the symmetric stretching mode.[20] Vallet et al. investigated in 2001 the structures of U(IV) fluoride and hydroxide complexes by extended X-ray absorption fine structure (EXAFS) spectroscopy as well as quantum chemical calculations using a relativistic U small-core ECP combined with hybrid DFT (B3LYP) and single-point Møller–Plesset second-order perturbation theory (MP2).[21] Both implicit modelling and explicit modelling of hydration effects was investigated. The explicit inclusion of the second aquo solvation sphere of the investigated $[UO_2(H_2O)_{5-n}F_n]^{2-n}$ (n = 3–5) complexes was found to be essential to obtain accurate results. Mixed uranyl aquo fluoro complexes $[UO_2(H_2O)_xF_y]^{2-y}$ (y = 1–4, $x + y$ = 4, 5) were investigated in the gas phase as well as in aqueous solution by Bühl et al. in 2009 using gradient-corrected DFT (BLYP) in the framework of Car–Parrinello molecular dynamics (CPMD[22]) simulations.[23] The number of equatorial ligands on UO_2^{2+} was found to be difficult to establish. Among the fivefold coordinated complexes only $[UO_2(H_2O)_4F]^+$ and $[UO_2(H_2O)_3F_2]$ were found to be stable (or metastable) for a few picoseconds in the gas phase in unconstrained CPMD simulations, whereas all other investigated complexes rearranged to species with lower coordination numbers. The CPMD results reproduced the free binding energy of fluorine in $[UO_2(H_2O)_4F]^+$ in aqueous solution within 1 kcal mol^{-1} of the published experimental value, whereas $[UO_2(H_2O)_3F_2]$ was found

to be unstable against a loss of water. Accompanying static gradient-corrected (BLYP) and hybrid (B3LYP) DFT calculations using a U small-core ECP led the authors to conclude that the affinity of $[UO_2F_4]^{2-}$ to accommodate H_2O as a fifth equatorial ligand is lower than that assumed previously. Further theoretical and experimental investigations were recommended. Finally, in 2011 Odoh et al. studied the structural and electronic properties of $[UO_2(H_2O)_{5-n}F_n]^{2-n}$ (n = 0–5) in the gas phase and aqueous solution modeled using the conductor-like screening model (COSMO)[24] using a U small-core ECP, the QR AE zeroth-order regular approximation (ZORA) and gradient-corrected as well as hybrid DFT (BP86, B3LYP).[25] Similar to previous studies they found that the implicit modeling of hydration by COSMO, or a polarizable continuum model (PCM), is not sufficient to obtain accurate U=O bond distances, fluoride binding energies and UO_2^{2+} vibrational frequencies. Addition of five explicitly treated water molecules to the second coordination sphere of $[UO_2(H_2O)_5]^{2+}$ and $[UO_2F_5]^{3-}$, i.e., explicitly taking into account hydrogen bonding between the first and second coordination spheres, brought the calculated symmetric stretching frequencies (878 and 799 cm^{-1}) into good agreement with the experimental values (870 and 784 cm^{-1}), whereas the implicit modeling only with COSMO leads to inferior values (898 and 753 cm^{-1}). Similarly, the slope of the nearly linear variation of the U=O bond distances with the number n of fluoride ligands is reduced by roughly a factor of two when replacing the COSMO modeling of hydration by an explicit treatment water in the second coordination sphere combined with COSMO representing the bulk water, bringing the variation between n = 0 and n = 5 from about 0.08 Å down to 0.04 Å in good agreement with experimental evidence. However, a systematic theoretical investigation of the whole series of uranyl complexes $[UO_2(H_2O)_{5-n}F_n]_{2-n}$ (n = 0–5) in aqueous solution taking explicitly into account the second coordination sphere, especially considering the effects on the characteristic UO_2^{2+} stretching frequencies and U=O bond distances, is still missing. In particular wavefunction-based ab initio approaches have not been applied to the best of our knowledge to evaluate these characteristic quantities.

We have therefore decided to systematically study the thermodynamic properties and structural characteristics of uranyl complexes with fluoride in aqueous solutions by combining Raman spectrometry and relativistic quantum chemical methods. First, the titrations of UO_2^{2+} with F^- were conducted by monitoring the variation in Raman spectroscopy. Second, the formation constants and molar normalized intensities of single components were calculated by the deconvolution of titration spectra. Third, the vibrational bands involved in the Raman spectra were analyzed aiming at a structure-to-signal correlation. Finally, extensive electronic structure calculations for a rather complete series of $[UO_2(H_2O)_mF_n]^{2-n}(H_2O)_k$ (n = 0–5) complexes in the gas phase (k = 0) as well as in aqueous solution ($k \geq 0$) modelling bulk water using the COSMO approach were performed. These studies also provided accurate data for the $UO_2F_5^{3-}$ complex, which was observed here for the first time but could not be investigated in detail experimentally. To the best of our knowledge the quantum chemical study presented here is not only the most complete for the $UO_2^{2+}/F^-/H_2O$ system but

This journal is © the Owner Societies 2024

Phys. Chem. Chem. Phys., 2024, **26**, 18584–18591 | **18585**

also the first to present structures and vibrational frequencies at the *ab initio* level. The latter aspect as well as the explicit modeling of the second coordination sphere was found to be crucial for obtaining good agreement with the experimental results presented here.

The complexation of uranyl UO_2^{2+} with fluoride in aqueous solution was previously studied by one of the present authors using spectrophotometry.[26] Four successive complexes UO_2F^+, $UO_2F_2(aq)$, $UO_2F_3^-$ and $UO_2F_4^{2-}$ were identified using UV/vis absorption spectroscopy in the wavelength region between 380 and 480 nm. Their stability was found to increase when the temperature was elevated in the region between 25 and 70 °C. Based on microcalometric titrations with NaF/HF the complexation of UO_2^{2+} with fluoride was analyzed to be slightly endothermic and entropy-driven. Our present study combines advanced experimental and theoretical techniques to obtain a better understanding of the $UO_2^{2+}/F^-/H_2O$ system.

2. Experimental

2.1. Chemicals

All chemicals except for uranium were reagent grade or higher. Deionized water from a Milli-Q system was used in the preparation of all solutions. A stock solution of $UO_2(NO_3)_2$ was prepared by dissolving $UO_2(NO_3)_2 \cdot 6H_2O$ directly. For preparing a $UO_2(ClO_4)_2$ stock solution, $Na_2U_2O_7$ was precipitated from a $UO_2(NO_3)_2$ solution by adding excess of NaOH and washed three times with deionized water, and then the precipitate was dissolved with concentrated perchloric acid (70%) under stirring and diluted with water. The concentrations of U(vi) and perchlorate were determined by Raman spectrophotometry using nitrate as internal standard and the concentration of free H^+ was calculated by the law of charge conservation. A stock solution of NaF (0.9 M) was prepared by directly dissolving NaF in Milli-Q water.

2.2. Spectrophotometry

The present investigation of metal-bonding equilibrium was carried out as a series of Raman spectral titrations. For a typical titration, 75 μL of $UO_2(ClO_4)_2$ solutions were placed in a set of centrifuge tubes, and then different aliquots of 0.9 M NaF solutions were added into each tube and diluted to 1 mL. Furthermore, $UO_2(ClO_4)_2$ and NaF were replaced by $UO_2(NO_3)_2$ and $(CH_3)_4NF$ to increase the F^- level. All the solutions were mixed thoroughly (for 1–2 min) and maintained at 25.0 °C ± 0.1 °C through a circulating water bath before the spectra were collected.

Raman spectra were acquired on a Renishaw inVia Raman micro-spectrometer at a nominal resolution of 1.4 cm^{-1} in the range of 800–1100 cm^{-1}. A diode laser (532 nm line) was used as the excitation source. The excitation light with a maximum laser power of 20 mW was focused on samples by using the microscope. The exposure time was 20 s and the number of scans was 30 in all measurements.

In the titration of $UO_2(ClO_4)_2$ with NaF, the same concentration of perchlorate was kept in the samples, so all the spectra were normalized to the molar intensity of perchlorate. Similarly, all the spectra were normalized to the molar intensity of nitrate during the titration of $UO_2(NO_3)_2$ with $(CH_3)_4NF$.[14] The formation constants and the Raman spectra of the U(vi)/F^- complexes were calculated, from the normalized Raman spectral data in the range of 750–950 cm^{-1}, with the HypSpec 2013 program.

2.3. Quantum chemistry

Quantum chemical *ab initio* and first principles calculations were performed with the electronic structure codes GAUSSIAN,[27] MOLPRO[28,29] and TURBOMOLE.[30] A scalar-relativistic energy-adjusted small-core pseudopotential (ECP60MWB[31]) and a corresponding (14s13p10d8f6g)/[10s9p5d4f3g] basis set[32] of polarized valence-quadruple-zeta quality were used for U in order to account for the leading relativistic contributions. H, O and F were described by def2-TZVPP basis sets, *i.e.*, (11s6p2d1f)/[5s3p2d1f] for O and F, and (5s2p1d)/[3s2p1d] for H.[33] Calculations including electron correlation effects were performed with the gradient-corrected B3LYP hybrid density functional[25] and at the second-order level of Møller–Plesset perturbation theory (MP2). Bulk hydration effects were described by the conductor-like screening model (COSMO[24]) using a dielectric constant $\varepsilon = 78$. For the cavity generation in our calculations the following atomic radii (Å) were adopted from the default values implemented in TURBOMOLE: O (1.72), H (1.3), and U (2.223). Geometry optimizations were performed for the complexes in the gas phase as well as in aqueous solution. All minimum structures were confirmed by $3N - 6$ real positive eigenvalues of the Hessian matrix (N: number of atoms), except for the $[UO_2(H_2O)_3F_2](H_2O)_4$ complex at the MP2 level in aqueous solution modeled by COSMO, where one imaginary value of 7.52i cm^{-1} was found in the numerical frequency evaluation (*cf.* ESI†). The following notation is used: ligands of UO_2^{2+} in the first coordination sphere are given inside the brackets, whereas additional explicitly treated water molecules in the second coordination sphere are listed outside the brackets, *i.e.*, $[UO_2^{2+}(H_2O)_mF_n]^{2-n}(H_2O)_k$. Note that for a specific first coordination sphere (a given pair n, m) an infinite number k of water molecules could be added to the second and subsequent coordination spheres, forming hydrogen bonds to the n fluoride and m water ligands as well as to the uranyl oxygens. We found in several test calculations that only those water molecules which form hydrogen bonds to the fluoride ligands in the first coordination sphere have a significant effect on the UO_2^{2+} bond distances as well as the uranyl vibrational stretching frequencies (*cf.* ESI†). We therefore restricted our study to such cases, thus in practice limiting, also due to steric requirements, the number k of explicitly treated additional water molecules to at most five, whereas treating bulk water with the COSMO approach. We further considered only cases where all fluoride ligands have at least one hydrogen bond to an explicitly treated water molecule. Since according to our observations each fluoride ligand forms at most two hydrogen bonds in energetically favorable arrangements, a rule of thumb $n \le k \le \min(2n, 5)$ for constructing the investigated $[UO_2^{2+}(H_2O)_mF_n]^{2-n}(H_2O)_k$ complexes results. The Cartesian coordinates of the energetically lowest complexes for given triples n, m, k found by applying these assumptions are given in the ESI.†

18586 | *Phys. Chem. Chem. Phys.*, 2024, **26**, 18584–18591

This journal is © the Owner Societies 2024

3. Results and discussion

3.1. Raman spectra of UO_2^{2+} titrated with F^-

Fig. 1 shows Raman spectra of representative spectrophotometric titrations of $UO_2(ClO_4)_2$ with NaF. With the addition of the NaF titrant solution, the intensities of the Raman band at 870 cm^{-1} that belongs to the free UO_2^{2+} cation decreased and a new band appeared at 858 cm^{-1}, which is ascribed to the formation of a 1:1 complex of U(VI) with F^-, UO_2F^+. With addition of more titrant solution, successive bands wax and wane at 858 cm^{-1}, 848 cm^{-1}, 837 cm^{-1}, and 828 cm^{-1}. The three new bands at lower frequencies were assigned to the $UO_2F_2(aq)$, $UO_2F_3^-$, and $UO_2F_4^{2-}$ species, respectively. The band at 828 cm^{-1} was the last one observed in the U(VI)/NaF system of 1 M ion strength in which the highest F^- concentration that could be achieved is about 0.54 M. The calculated formation constants of the 1:1, 1:2, 1:3, and 1:4 complexes ($\log \beta_1$, $\log \beta_2$, $\log \beta_3$, and $\log \beta_4$) are 4.32 ± 0.18, 7.50 ± 0.36, 9.74 ± 0.45, and 10.80 ± 0.5, respectively, which are in good agreement with the values in the literature.[26]

Though the $UO_2F_5^{3-}$ species was not identified in $UO_2(ClO_4)_2$–NaF solutions, with more soluble tetramethyl ammonium fluoride instead of NaF as the titrant, continuous shift to wavenumbers lower than 828 cm^{-1} was observed, which was ascribed to the formation of the 1:5 complex $UO_2F_5^{3-}$, Fig. 2. Every Raman spectrum of the uranyl moiety obtained in high $(CH_3)_4NF$ concentrations consists of contributions from two species: $UO_2F_4^{2-}$ at 828 cm^{-1} and $UO_2F_5^{3-}$ at 817 cm^{-1}. As the concentration of $(CH_3)_4NF$ increased, intensities of the Raman band of $UO_2F_4^{2-}$ decreased and the intensities of the Raman band of $UO_2F_5^{3-}$ increased. The calculated stepwise formation constant of the $UO_2F_5^{3-}$ complexes (K_5) is 0.92, as shown in the ESI,† Table S1, and is calculated on the basis of the molar normalized intensity of the $UO_2F_4^{2-}$ complex (Fig. 1) and the total concentrations of UO_2^{2+} and $(CH_3)_4NF$ that were added to the solution initially.

Nguyen-Trung et al. proposed a linear correlation between the symmetrical stretching frequency ν_1 for the uranyl ion and the number of ligands coordinated in the equatorial plane of uranyl, commonly symbolized as $\bar{n}$, in eqn (1). Among them, the origin is UO_2^{2+}, with ν_1 = 870 cm^{-1} and $\bar{n}$ = 0.[20]

$$\nu_1 \ (cm^{-1}) = -A\bar{n} + 870 \ cm^{-1} \tag{1}$$

In the present work, five fluoride complexes have been identified by spectral titration. A plot of $\bar{n}$ versus the six frequencies observed in NaF and $(CH_3)_4NF$ solutions is linear with slope $A = 10.5 \pm 1 \ cm^{-1}$ when the stepwise shifts in the frequency are assigned to UO_2^{2+}, UO_2F^+, $UO_2F_2(aq)$, $UO_2F_3^-$, $UO_2F_4^{2-}$ and $UO_2F_5^{3-}$, respectively, that is, the average difference in vibrational energies between successive complexes being 10.5 cm^{-1}. However, there are some differences in speciation and frequencies between the present work and the literature.[20] In the previous research, the $UO_2F_5^{3-}$ complex was not identified in NaF and $(CH_3)_4NF$ solutions, but only four new bands at 858 cm^{-1}, 848 cm^{-1}, 834 cm^{-1}, and 822 cm^{-1}, respectively, assigned to UO_2F^+, $UO_2F_2(aq)$, $UO_2F_3^-$, and $UO_2F_4^{2-}$, were reported. Besides, the average difference in vibrational energies between successive complexes is 12 cm^{-1}. Among these bands,
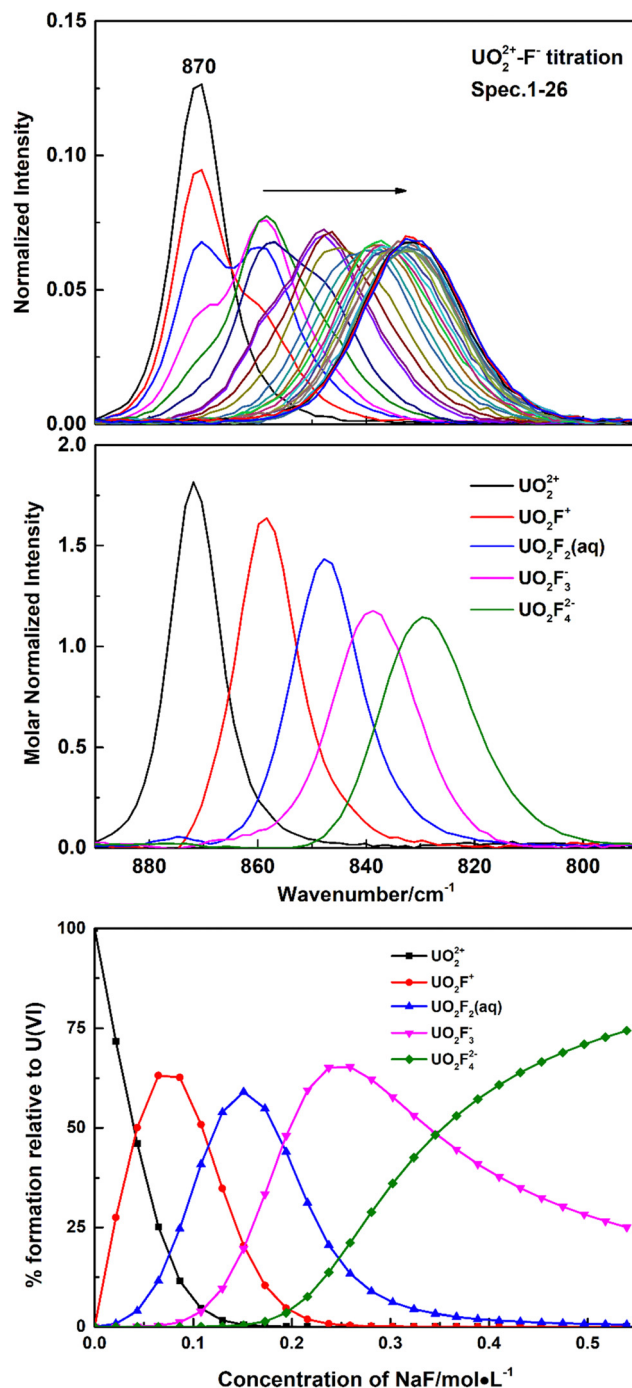

Fig. 1 Representative Raman spectral titration of U(VI) with fluoride. Top: Spectra collected during a titration (normalized to the intensity of 0.257 M perchlorate). Middle: Raman spectra of U(VI)/fluoride complexes of relative intensity from deconvolution. C_{uranyl} = 0.074 M, $C_{perchlorate}$ = 0.257 M, V = 0.66 mL, C_{H^+} = 0.003 M, $C_{fluoride}$ = 0–0.54 M. Bottom: Speciation distribution during the titration.

the first two bands around 858 cm^{-1} and 847 cm^{-1} are observed in the literature and the present work, but the frequencies corresponding to $UO_2F_3^-$ and $UO_2F_4^{2-}$ are different. It is obvious that the frequencies of $UO_2F_3^-$ and $UO_2F_4^{2-}$ deconvoluted from Raman spectra during titration in the present work, 837 cm^{-1}

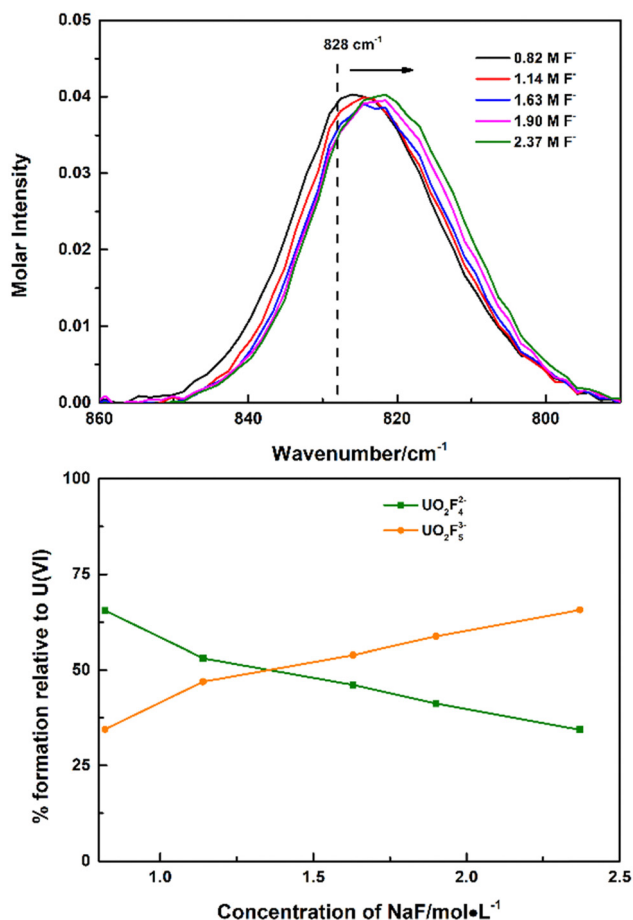This journal is © the Owner Societies 2024

Phys. Chem. Chem. Phys., 2024, **26**, 18584–18591 | **18587**

Fig. 2 Raman spectra of $UO_2(NO_3)_2$ in 2.5 M $(CH_3)_4NNO_3/(CH_3)_4NNO_3$ (top) and speciation distribution during titration (bottom). C_{uranyl} = 0.059 M, $C_{nitrate}$ = 0.118–1.69 M, V = 1.0 mL, C_{H^+} = 0.002 M, $C_{fluoride}$ = 0.82–2.37 M.

and 828 cm^{-1}, by 3 cm^{-1} and 6 cm^{-1}, respectively, higher than those reported in the literature (834 cm^{-1} and 822 cm^{-1}). Considering that there is no observation of an old band disappearing or a new band appearing, only a continuous shift was detected at high NaF and $(CH_3)_4NF$ concentrations, and it is difficult to accurately interpret slight variations of spectra and speciation of $UO_2F_3^-$, $UO_2F_4^{2-}$, and $UO_2F_5^{3-}$ complexes by simple curve fitting. However, with the application of Raman spectral titration, the calculated molar normalized spectrum of $UO_2F_n^{2-n}$ can be strictly limited by formation constants of the $UO_2F_n^{2-n}$ complex, providing a more reasonable assignment in the present work. As suggested above, it is the first time the $UO_2F_5^{3-}$ complex is identified, with a symmetric vibrational stretching frequency at 817 cm^{-1}.

3.2. Structures and vibrational frequencies from quantum chemistry

The Cartesian coordinates and the total energies of the optimized B3LYP and MP2 equilibrium structures of selected complexes $[UO_2(H_2O)_mF_n]^{2-n}(H_2O)_k$ in aqueous solution modeled by COSMO are provided in the ESI.† Listings with U=O

distances and the frequencies of the symmetric UO_2^{2+} stretching vibrations are also provided for all complexes in the gas phase and in solution (COSMO), both at the B3LYP and MP2 levels of theory.

Table 1 lists U=O bond distances and UO_2^{2+} symmetric stretching frequencies for selected more stable $[UO_2(H_2O)_mF_n]^{2-n}$ complexes in the gas phase at the B3LYP level. The O of the H_2O ligands is coordinated directly to the U center. The F$^-$ ions obviously donate more electron density to antibonding orbitals of UO_2^{2+} than H_2O, so that upon replacing H_2O by F$^-$ the U=O bond distance becomes significantly longer and the symmetric stretching frequency becomes drastically smaller, i.e., by about 0.1 Å and almost 200 cm^{-1} when going from $[UO_2(H_2O)_5]^{2+}$ to $[UO_2F_5]^{3-}$. These results are in stark contrast, e.g., to the Raman data reported above, where a decrease from 870 cm^{-1} to 828 cm^{-1} was associated with the series of hydrated complexes from $[UO_2(H_2O)_5]^{2+}$ to $[UO_2F_4]^{2-}$, i.e., a lowering of only about 10 cm^{-1} per H_2O–F$^-$ exchange.

Taking bulk hydration effects into account by the COSMO approach at the B3LYP level does not improve the situation much. The symmetric stretching frequencies range from 912 cm^{-1} to 769 cm^{-1} for the series of complexes listed in Table S2 of the ESI.† When applying the *ab initio* approach MP2 combined with COSMO, a symmetric stretching frequency of 881 cm^{-1} is obtained for $[UO_2(H_2O)_5]^{2+}$ (Table S2, ESI†), in quite good agreement with the present experimental value of 870 cm^{-1} and an older one of 874 cm^{-1}.[34] However, the corresponding results of 795 cm^{-1} and 777 cm^{-1} for $[UO_2(H_2O)F_4]^{2-}$ and $[UO_2F_5]^{3-}$ are still much too low compared to the measured and extrapolated experimental values of 828 cm^{-1} and 817 cm^{-1}, respectively.

Considering $[UO_2(H_2O)_mF_n]^{2-n}(H_2O)_k$ complexes in bulk water modeled by COSMO, i.e. k additional H_2O molecules in the second coordination sphere, which are not directly bonded to U, but rather form hydrogen bonds to the F$^-$ ligands, the results are improved a lot. For example, the MP2 result in COSMO for a $[UO_2F_5]^{3-}(H_2O)_5$ is 818 cm^{-1} in excellent agreement with the extrapolated experimental value of 817 cm^{-1}. Similarly, for $[UO_2F_4]^{2-}(H_2O)_4$ a value of 819 cm^{-1} is calculated, compared to a measured one of 828 cm^{-1}. Such improvements are also observed for the complexes with one to three F$^-$ ligands, although not always the number of H_2O molecules building hydrogen bridges to the F$^-$ ligands can be determined unambiguously, cf. Table 2. These additional water molecules

Table 1 U=O bond distances (Å) and UO_2^{2+} symmetric stretching frequencies (cm^{-1}) from B3LYP gas phase calculations of $[UO_2(H_2O)_mF_n]^{2-n}$ complexes with H_2O directly coordinated to U

Complex	R(U=O)	ω_e
$[UO_2(H_2O)_5]^{2+}$	1.739	948
$[UO_2(H_2O)_4F]^+$	1.761	904
$[UO_2(H_2O)_3F_2]_{meta}$	1.775	874
$[UO_2(H_2O)_2F_3]_{ortho}^-$	1.790	838
$[UO_2(H_2O)_2F_3]^-$	1.790	833
$[UO_2F_4]^{2-}$	1.819	794
$[UO_2F_5]^{3-}$	1.834	756

18588 | *Phys. Chem. Chem. Phys.*, 2024, **26**, 18584–18591

This journal is © the Owner Societies 2024

Table 2 UO_2^{2+} symmetric stretching frequencies (cm^{-1}) from MP2 COSMO calculations of $[UO_2(H_2O)_mF_n]^{2-n}(H_2O)_k$ complexes in comparison to Raman data for aqueous solution. The additional k H_2O molecules form hydrogen bridges to the F^- ligands

Complex	MP2, COSMO	Raman
$[UO_2(H_2O)_5]^{2+}$	881	870
$[UO_2(H_2O)_4F]^+(H_2O)$	860	858
$[UO_2(H_2O)_4F]^+(H_2O)_2$	863	858
$[UO_2(H_2O)_3F_2](H_2O)_{3\ ortho}$	848	848
$[UO_2(H_2O)_3F_2](H_2O)_{4\ meta}$	850	848
$[UO_2(H_2O)F_3]^-(H_2O)_4$	837	837
$[UO_2F_4]^{2-}(H_2O)_4$	819	828
$[UO_2F_5]^{3-}(H_2O)_5$	818	817^a

^{a} Extrapolated Raman value.

prohibit the F^- ligands from donating too strong electron density to antibonding UO_2^{2+} orbitals, so that besides higher symmetric stretching frequencies also somewhat shorter U=O bond distances result. For example, at the MP2/COSMO level a U=O bond distance of 1.826 Å for $[UO_2F_5]^{3-}$ is reduced to 1.795 Å for $[UO_2F_5]^{3-}(H_2O)_5$.

Fig. 3 shows the nearly linear dependence of the symmetric UO_2^{2+} stretching frequencies on the number of fluoride ligands. It is seen that MP2 calculations neither for the gas phase nor for aqueous solution modeled solely by COSMO are in satisfactory agreement with experimental data, whereas the explicit inclusion of k water molecules in the second coordination sphere leads to an excellent agreement. Qualitatively, the behavior of the calculated B3LYP data is the same, although quantitatively the results are somewhat worse compared to that for MP2 (*cf.* Table S3 in the ESI†). Note that for $n = 0$ no water molecules in the second coordination sphere are treated explicitly in our model and only COSMO is applied. In this case the B3LYP symmetric UO_2^{2+} vibrational frequency of 912 cm^{-1} is significantly higher than the corresponding MP2 result of
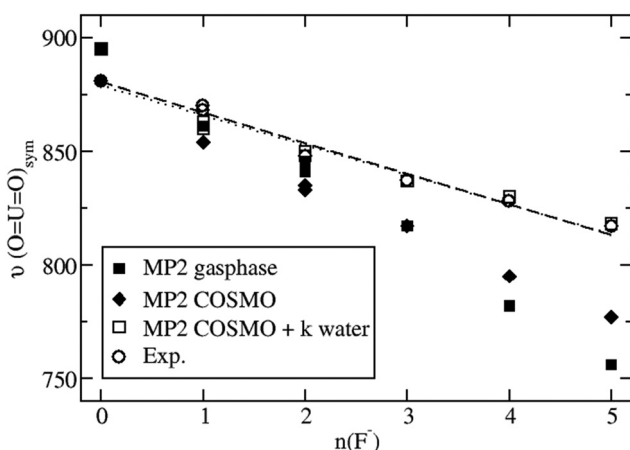
881 cm^{-1} and the two experimental values of 870 and 874 cm^{-1}. On the other hand for $n = 5$ five water molecules are treated explicitly in the second coordination sphere and the B3LYP and MP2 results of 817 cm^{-1} and 818 cm^{-1}, respectively, virtually agree with the extrapolated experimental value of 817 cm^{-1}. Thus the dependency of the results on the number of fluoride ligands is too strong for B3LYP and just about right for MP2.

Relativistic coupled cluster calculations (CCSD(T)) on the UO_2^{2+} cation showed that anharmonic effects decreased the vibrational frequencies, whereas spin–orbit effects increased the stretching frequencies and decreased the bending frequencies.[35] Overall these two corrections led to a decrease of the vibrational frequencies, *i.e.*, by 6 cm^{-1} for the asymmetric stretching mode, as well as by 3 cm^{-1} for the symmetric stretching and the bending modes. In view of these small corrections and the significantly more complex systems treated here we neglected both anharmonic effects as well as spin–orbit coupling in the present work. We are confident that these small corrections would not affect the general trends and main conclusions of our work.

Concerning the newly found $UO_2F_5^{3-}$ complex we note that at the level of computation applied here this system is unstable in the gas phase both to the loss of an electron as well as to the loss of a fluoride ion F^-, whereas it is stable in aqueous solution. In particular, based on total energies at the MP2 level using the COSMO approach $[UO_2F_5]^{3-}$ is about 21.2 kJ mol^{-1} more stable than its dissociation products $[UO_2F_5]^{2-} + F^-$. On the experimental side it seems to be likely that in previous studies there was a certain amount of $UO_2F_5^{3-}$ in the solution as the concentration of F^- has been increased to 1.0 M; however, only two bands at 834 cm^{-1} and 822 cm^{-1}, which were assigned to $UO_2F_3^-$ and $UO_2F_4^{2-}$, respectively, have been identified by simple curve fitting, and the formation of $UO_2F_5^{3-}$ was not considered. In the present work, the deconvolution of the Raman spectra for UO_2^{2+}, UO_2F^+, $UO_2F_2(aq)$, $UO_2F_3^-$ and $UO_2F_4^{2-}$ was strictly limited by chemometrics and formation constants. As a result, it is more reasonable to assign Raman bands at 837 cm^{-1} and 828 cm^{-1}, which were calculated from deconvolution, to the symmetrical stretching modes of $UO_2F_3^-$ and $UO_2F_4^{2-}$, respectively. Only the Raman band of $UO_2F_5^{3-}$ was calculated from curve fitting at high fluoride concentration.

Fig. 3 Symmetric UO_2^{2+} stretching frequencies $\upsilon(O=U=O)_{sym}$ of $[UO_2(H_2O)_mF_n]^{2-n}$ complexes depending on the number $n(F^-)$ of fluoride ligands. MP2 results for the gas phase and aqueous solution, modeled by COSMO as well as k explicitly treated water molecules and COSMO, in comparison to experimental values. The nearly linear dependence is illustrated by dashed and dotted lines for the MP2 COSMO + k water and experimental data sets, respectively.

4. Conclusions

In this work, the thermodynamic properties and structural characteristics for five uranyl fluoride complexes in aqueous solution are investigated by combining Raman spectrometry and quantum chemical calculations. The titrations of UO_2^{2+} with F^- were conducted by monitoring the variation in Raman spectroscopy. The formation constants and molar scattering intensities of single components were calculated by the deconvolution of the titration spectra. Furthermore, quantum chemical *ab initio* calculations at the MP2 level including relativistic contributions originating from U as well as bulk hydration effects yield frequencies in good agreement with

This journal is © the Owner Societies 2024

Phys. Chem. Chem. Phys., 2024, **26**, 18584–18591 | **18589**

experimental data only if water molecules in the second coordination sphere are explicitly taken into account. The formation constants, energy levels and structural information acquired as well as the developed modeling approach and quantum methodology could be beneficial to the future experimental and theoretical research on uranyl chemistry.

Conflicts of interest

There are no conflicts to declare.

Acknowledgements

References

1 E. Kraka, Uranium: The nuclear fuel cycle and beyond, *Int. J. Mol. Sci.*, 2022, **23**(9), 4655.

2 A. Y. Romanchuk, I. E. Vlasova and S. N. Kalmykov, Speciation of uranium and plutonium from nuclear legacy sites to the environment: A mini review, *Front. Chem.*, 2020, **8**, 630.

3 G. Tian, S. J. Teat and L. Rao, Thermodynamic studies of U(VI) complexation with glutardiamidoxime for sequestration of uranium from seawater, *Dalton Trans.*, 2013, **42**(16), 5690–5696.

4 G. Tian, S. J. Teat, Z. Zhang and L. Rao, Sequestering uranium from seawater: binding strength and modes of uranyl complexes with glutarimidedioxime, *Dalton Trans.*, 2012, **41**(38), 11579–11586.

5 Z. Zhang, G. Helms, S. B. Clark, G. Tian, P. L. Zanonato and L. Rao, Complexation of uranium(VI) by gluconate in acidic solutions: a thermodynamic study with structural analysis, *Inorg. Chem.*, 2009, **48**(8), 3814–3824.

6 L. Rao and G. Tian, Thermodynamic study of the complexation of uranium(VI) with nitrate at variable temperatures, *J. Chem. Thermodyn.*, 2008, **40**(6), 1001–1006.

7 C. Xu, G. Tian, S. J. Teat and L. Rao, Complexation of U(VI) with dipicolinic acid: Thermodynamics and coordination modes, *Inorg. Chem.*, 2013, **52**(5), 2750–2756.

8 G. Tian and L. Rao, Spectrophotometric and calorimetric studies of U(VI) complexation with sulfate at (25 to 70) °C, *J. Chem. Thermodyn.*, 2009, **41**(4), 569–574.

9 R. Xie, W. Johnson, S. Spayd, G. S. Hall and B. Buckley, Arsenic speciation analysis of human urine using ion exchange chromatography coupled to inductively coupled plasma mass spectrometry, *Anal. Chim. Acta*, 2006, **578**(2), 186–194.

10 H. Sodaye, S. Nisan, C. Poletiko, S. Prabhakar and P. K. Tewari, Extraction of uranium from the concentrated brine rejected by integrated nuclear desalination plants, *Desalination*, 2009, **235**(1), 9–32.

11 Z. F. Wang and Z. J. Cui, Supercritical fluid extraction and gas chromatography analysis of arsenic species from solid matrices, *Chin. Chem. Lett.*, 2016, **27**(2), 241–246.

12 F. Kou, S. Yang, H. Qian, L. Zhang, C. M. Beavers, S. J. Teat and G. Tian, A fluorescence study on the complexation of Sm(III), Eu(III) and Tb(III) with tetraalkyldiglycolamides (TRDGA) in aqueous solution, in solid state, and in solvent extraction, *Dalton Trans.*, 2016, **45**(46), 18484–18493.

13 F. Kou, S. Yang, L. Zhang, S. J. Teat and G. Tian, Complexation of Ho(III) with tetraalkyl-diglycolamide in aqueous solutions and a solid state compared in organic solutions of solvent extraction, *Inorg. Chem. Commun.*, 2016, **71**, 41–44.

14 Q. Liu, Q. Zhang, S. Yang, H. Zhu, Q. Liu and G. Tian, Raman spectral titration method: an informative technique for studying the complexation of uranyl with uranyl(VI)-DPA/oxalate systems as examples, *Dalton Trans.*, 2017, **46**(39), 13180–13187.

15 B. Drobot, A. Bauer, R. Steudtner, S. Tsushima, F. Bok, M. Patzschke, J. Raff and V. Brendler, Speciation studies of metals in trace concentrations: The mononuclear uranyl(VI) hydroxo complexes, *Anal. Chem.*, 2016, **88**(7), 3548–3555.

16 B. Drobot, R. Steudtner, J. Raff, G. Geipel, V. Brendler and S. Tsushima, Combining luminescence spectroscopy, parallel factor analysis and quantum chemistry to reveal metal speciation-a case study of uranyl(VI) hydrolysis, *Chem. Sci.*, 2015, **6**(2), 964–972.

17 A. D. Becke, Density-functional thermochemistry. I. The effect of the exchange-only gradient correction, *J. Chem. Phys.*, 1992, **96**(3), 2155–2160.

18 A. Becke, Density-functional thermochemistry. III. The role of exact exchange, *J. Chem. Phys.*, 1993, **98**(7), 5648–5652.

19 G. Schreckenbach, P. J. Hay and R. L. Martin, Density functional calculations on actinide compounds: Survey of recent progress and application to $[UO_2X_4]^{2-}$ (X = F, Cl, OH) and AnF_6 (An = U, Np, Pu), *J. Comput. Chem.*, 1999, **20**(1), 70–90.

20 C. Nguyen-Trung, G. M. Begun and D. A. Palmer, Aqueous uranium complexes. 2. Raman spectroscopic study of the complex formation of the dioxouranium(VI) ion with a variety of inorganic and organic ligands, *Inorg. Chem.*, 1992, **31**(25), 5280–5287.

21 V. Vallet, U. Wahlgren, B. Schimmelpfennig, H. Moll, Z. Szabo and I. Grenthe, Solvent effects on uranium(VI) fluoride and hydroxide complexes studied by EXAFS and quantum chemistry, *Inorg. Chem.*, 2001, **40**(14), 3516–3525.

22 R. Car and M. Parrinello, Unified approach for molecular dynamics and density-functional theory, *Phys. Rev. Lett.*, 1985, **55**(22), 2471.

23 M. Bühl, N. Sieffert and G. Wipff, Density functional study of aqueous uranyl(VI) fluoride complexes, *Chem. Phys. Lett.*, 2009, **467**(4–6), 287–293.

24 A. Klamt and G. Schüürmann, COSMO: a new approach to dielectric screening in solvents with explicit expressions for the screening energy and its gradient, *J. Chem. Soc., Perkin Trans. 1*, 1993, 799–805.

25 S. O. Odoh, S. M. Walker, M. Meier, J. r Stetefeld and G. Schreckenbach, QM and QM/MM studies of uranyl fluorides in the gas and aqueous phases and in the hydrophobic cavities of tetrabrachion, *Inorg. Chem.*, 2011, **50**(7), 3141–3152.

18590 | *Phys. Chem. Chem. Phys.*, 2024, **26**, 18584–18591

This journal is © the Owner Societies 2024

26 G. Tian and L. Rao, Effect of temperature on the complexation of uranium(VI) with fluoride in aqueous solutions, *Inorg. Chem.*, 2009, **48**(14), 6748–6754.

27 M. J. Frisch, G. W. Trucks and H. B. Schlegel, *Gaussian 16*, Wallingford, CT, 2016.

28 H. J. Werner, P. J. Knowles, G. Knizia, F. R. Manby and M. Schütz, Molpro: a general-purpose quantum chemistry program package, *Wiley Interdiscip. Rev.: Comput. Mol. Sci.*, 2012, **2**(2), 242–253.

29 H.-J. Werner, P. J. Knowles, F. R. Manby, J. A. Black, K. Doll, A. Heßelmann, D. Kats, A. Köhn, T. Korona and D. A. Kreplin, The Molpro quantum chemistry package, *J. Chem. Phys.*, 2020, **152**(14), 144107.

30 R. Ahlrichs, M. Bär, M. Häser, H. Horn and C. Kölmel, Electronic structure calculations on workstation computers: The program system turbomole, *Chem. Phys. Lett.*, 1989, **162**(3), 165–169.

31 W. Küchle, M. Dolg, H. Stoll and H. Preuss, Energy-adjusted pseudopotentials for the actinides. Parameter sets and test calculations for thorium and thorium monoxide, *J. Chem. Phys.*, 1994, **100**(10), 7535–7542.

32 X. Cao and M. Dolg, Segmented contraction scheme for small-core actinide pseudopotential basis sets, *THEOCHEM*, 2004, **673**(1–3), 203–209.

33 F. Weigend and R. Ahlrichs, Balanced basis sets of split valence, triple zeta valence and quadruple zeta valence quality for H to Rn: Design and assessment of accuracy, *Phys. Chem. Chem. Phys.*, 2005, **7**(18), 3297–3305.

34 M. Gal, P. Goggin and J. Mink, Vibrational spectroscopic studies of uranyl complexes in aqueous and non-aqueous solutions, *Spectrochim. Acta, Part A*, 1992, **48**(1), 121–132.

35 V. E. Jackson, R. Craciun, D. A. Dixon, K. A. Peterson and W. A. De Jong, Prediction of vibrational frequencies of UO_2^{2+} at the CCSD(T) level, *J. Phys. Chem. A*, 2008, **112**(17), 4095–4099.

This journal is © the Owner Societies 2024

Phys. Chem. Chem. Phys., 2024, **26**, 18584–18591 | 18591